JOURNAL OF GEOPHYSICAL RESEARCH, VOL. 92, NO. B8, PAGES 8157-8168, JULY 10, 1987

COMPUTATION OF THE GRAVITY VECTOR FROM TORSION BALANCE DATA IN SOUTHERN OHIO

D. Arabelos

Department of Geodesy and Surveying, University of Thessaloniki, Greece

C.C. Tscherning

Geodaetisk Institut, Geodetic Department I, Charlottenlund, Denmark

Abstract. The method of least squares collocation was used for gravity vector estimation from torsion balance measurements in southern Ohio. The results were dependent on the covariance function used and on the selection of a proper signal to noise ratio. Here a standard deviation of the noise of 10 EU (10^{-9} s^{-2}) gave the best results. Expressed in terms of standard deviations of observed minus predicted differences, the best results were 0.4 arc sec for deflections of the vertical and 2 mGal for gravity anomalies. This compares to signal standard deviations of 4 arc sec and 22 mGal for deflections and gravity anomalies, respectively.

1. Introduction

The collocation and similar optimal estimation techniques have been proposed as possible methods for gravity vector estimation from gravity gradiometer data (see, e.g., Jekeli (1985)). Since gravity gradiometer data are not yet available, the estimation procedures have only been tested using simulated data. However, the torsion balance delivers measurements of the same kind as the gradiometer, namely, linear combinations of second-order derivatives of the gravity potential (W).

Using torsion balance data, we may then demonstrate how least squares collocation (LSC) can be used for gravity vector estimation and also show what type of difficulties one may encounter while using the method.

In order to draw conclusions from the use of torsion balance versus to the use of gravity gradiometer data, the data distribution should correspond to the one planned for the gradiometer. Furthermore, gravity vector data must also be available in the same area as the torsion balance data. Such an optimal situation is found in a 0.25° x 0.75° area in southern Ohio, where gravity data and deflections of the vertical and torsion balance data were observed and collected prior to 1970. The data are somewhat sparser than the ones planned for gradiometry, and the area covered is smaller than the typical area forseen to be covered by some hours of aerial gradiometer measurements. Furthermore, the observations are not performed at altitude but at ground level. Also, southern Ohio is not typical, since the area has no large height variations. However, in an operational situation, topographic effects will, in general, have to be removed (and restored). In this way, from the standpoint of the gravity field variation, all areas will look like Ohio (Forsberg, 1984, Table 6). Also the gravity variation at an altitude of 0.5-2.0 km will not be much different from the variation at ground level when topographic effects have been removed. Furthermore, as we shall see, an increase in the data density would probably not have improved the quality of the prediction vector.

The estimation of deflection of the vertical has been successfully tested in southern Ohio by Badekas and Mueller (1968), using a simple numerical integration method. With LSC we should be (and have been) able to obtain similar results, the advantage being that the method not only enables the estimation of the gravity vector at points where the measurements have been made but also at all points within a certain distance from the measurements. LSC permits the estimation of the prediction error as well.

In section 2 we will introduce the available data, and in section 3 we will describe the use of LSC and the associated process of estimating the so-called empirical covariance function. The results obtained using various combinations of the data as well as different analytic models for the empirical covariance function are described in section 4.

2. Southern Ohio Test Data Set

Let W be the gravity potential and U a corresponding reference (normal)potential. Then the anomalous gravity potential is the difference T = W - U.

The long-wavelength part of W (or T) is described down to a 1° resolution by one of the available spherical harmonic expansions complete to degree and order N=180, such as the OSU81 and the GPM2 coefficient sets (see Rapp, 1981; Wenzel, 1985).

Paper number 6B6308.
0148-0227/87/006B-6308$05.00

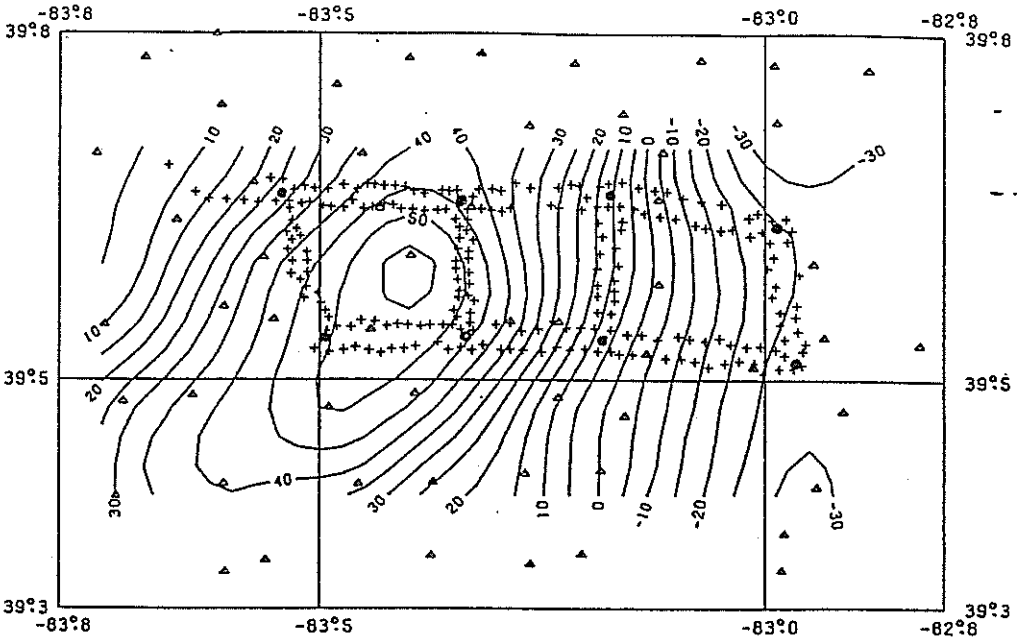

Fig. 1. The distribution of the torsion balance (pluses),gravity data (triangles) and deflections of the vertical (circles), with the free air gravity anomaly field contoured at 5 mGal interval.

Free air gravity anomalies (Δg) have been published by Heiskanen and Uotila (1956), and deflections of the vertical (ξ,η) have been published by Mueller and Preuss (1965). They are spherically approximated in relation to T through the following equations (Heiskanen and Moritz, 1967):

$$\Delta g = -\frac{\partial T}{\partial r} - \frac{2}{r} T \qquad (1)$$

$$\xi = -\frac{1}{r\gamma}\frac{\partial T}{\partial \phi} \qquad (2)$$

$$\eta = -\frac{1}{r\cos\phi\gamma}\frac{\partial T}{\partial \lambda} \qquad (3)$$

TABLE 1. Statistical Characteristics of the Raw and Reduced Data

		Raw Data		Data GPM2		Data GPM2 Topography	
		Mean	Standard Deviation	Mean	Standard Deviation	Mean	Standard Deviation
Δg,*	mGal	-1.24	22.20	-3.32	19.81	-3.32	16.74
Δg,**	mGal	22.64	27.66	16.31	25.98	16.24	22.41
ξ,	arc sec	0.92	1.44	0.98	1.49	-0.12	1.70
η,	arc sec	4.41	4.72	4.84	4.74	5.89	4.71
T_{xz},	EU	0.56	16.20	-0.52	16.24	-1.07	14.74
T_{yz},	EU	-8.69	20.59	-8.73	20.63	-7.89	19.40
T_{Δ},	EU	-0.35	22.62	-0.37	22.65	-1.12	20.10
$2*T_{xy}$,	EU	2.38	19.70	2.38	19.74	2.43	17.53

There are 227 gravity points, 12 gravity points, eight pairs of deflections of the vertical, and 233 points of torsion balance observations.

* 227 points.
** 12 points.

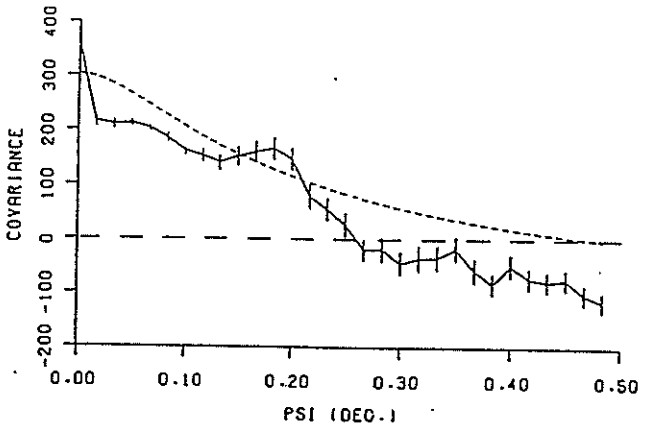

Fig. 2. Empirical (solid curve) and synthetic (dashed curve) covariance functions for the gravity anomalies in southern Ohio. GPM2 removed from the original data. Units $mGal^2$.

where ϕ is the latitude, λ the longitude, γ the normal gravity and r, the distance from the origin, which in the spherical approximation is obtained as the sum of the earth mean radius and the height. Torsion balance data are published by Badekas (1967), and their relations to T are

$$T_{xz} = \frac{\partial^2 T}{\partial x \partial z} \quad (4)$$

$$T_{yz} = \frac{\partial^2 T}{\partial y \partial z} \quad (5)$$

$$2T_{xy} = 2\,\frac{\partial^2 T}{\partial x \partial y} \quad (6)$$

$$T_{\Delta} = \frac{\partial^2 T}{\partial y^2} - \frac{\partial^2 T}{\partial x^2} \quad (7)$$

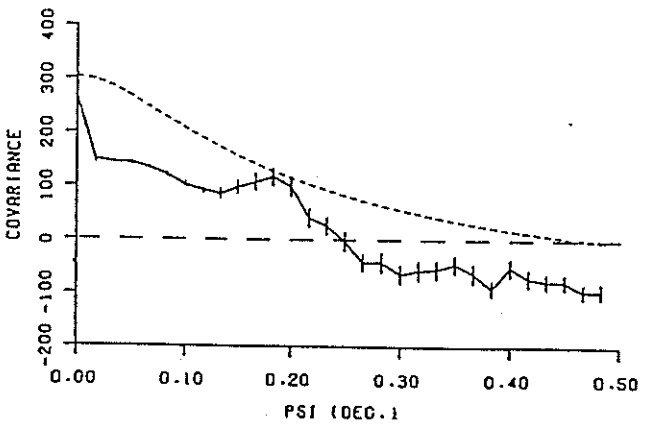

Fig. 3. Empirical and synthetic covariance functions for the gravity anomalies in southern Ohio. GPM2 and topographic (simple Bouguer plate) effect removed from the original data. Units $mGal^2$.

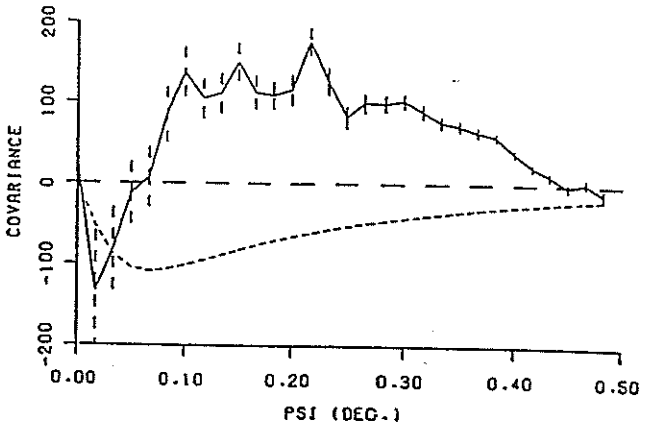

Fig. 4. Empirical and synthetic cross-covariance functions between Δg and T_{xz}. Units mGalxEU.

where (x,y,z) are the coordinates of a local level coordinate system with x east, y north, and z up. The distribution of the torsion balance data is shown in Figure 1.

Digital topographic heights were not available. However, topographic effects have been published for the torsion balance in the same publication as the observations and for the deflections of Badekas and Mueller (1968). The topographic effects on the gravity data may be calculated using the simple Bouguer plate reduction, since the terrain corrections are rather small due to the smooth topography.

The use of the spherical harmonic coefficients within the framework of LSC is equivalent to subtracting the contribution of the coefficients from the data. Since the data used for the determination of the coefficients primarily are free air gravity anomalies, the coefficients also represent the attraction of the topographic masses down to 1° resolution. Hence by subtracting the contribution

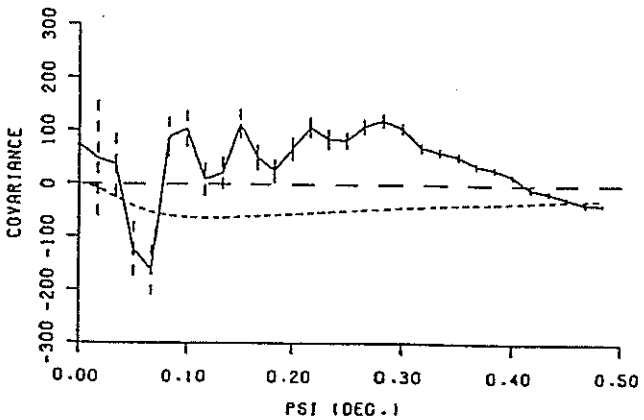

Fig. 5. Empirical and synthetic cross-covariance functions between Δg and T_{Δ}. Units mGalxEU.

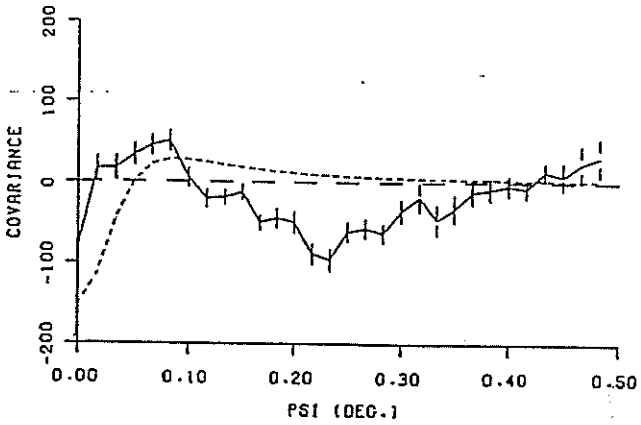

Fig. 6. Empirical and synthetic cross-covariance functions between $2*T_{xy}$ and T_{Δ}. Units EU^2.

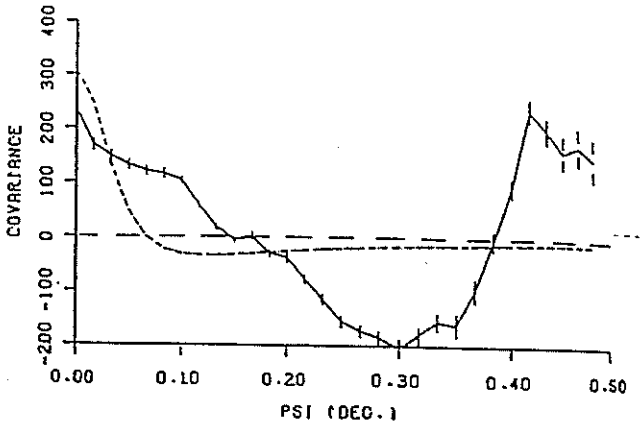

Fig. 8. Empirical and synthetic auto-covariance functions for the T_{xz} component. Units EU^2.

from the spherical harmonic coefficients, the topographic effects corresponding to a 1^{o} average topography are simultaneously subtracted. Consequently, only the attraction of the topography referring to the mean altitude of the topography (265 m) must be subtracted from the gravity anomalies. However, this creates an inconsistency between the topographic corrections for the gravity data and for the other data types, which as we shall see later will result in biases in the predicted results using topographically reduced data. This problem is easily avoided in practice if a detailed topographic model is available.

Table 1 shows the statistical characteristics of (1) the "raw" data, (2) the data from which the contribution from a set of spherical harmonic coefficients (GPM2 to maximum degree 180) have been subtracted and (3) the data of point 2 minus the topographic effects. Also statistics for a subset of the gravity data located in an area close to the torsion balance data are given in Table 1. These 12 gravity values have also been used in the tests described in section 4 when comparing observed and predicted quantities.

Note the striking difference in the mean values. In fact, the area is located on the top and east of a large anomalous mass. Also note that the deflections of the vertical have been transformed from NAD1927 to the preliminary NAD83 using datum shifts parameters provided by the U.S. National Geodetic Survey. The gravity values have been transformed from the Potsdam system to GRS1980 using a bias correction of 13.7 mGal. Hence a small bias with respect to IGSN 1971 may still be left.

3. Least Squares Collocation and Covariance Functions

The theory and practice of LSC is described in numerous publications. A recent survey is given by Tscherning (1985b).

Suppose that we have given n observations related to the anomalous gravity

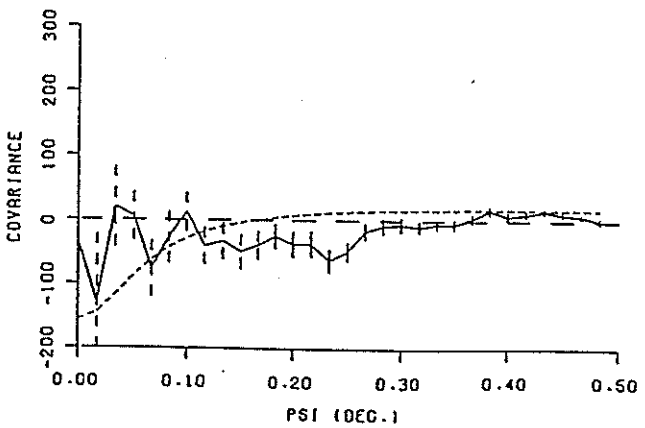

Fig. 7. Empirical and synthetic cross-covariance functions between Δg and $2*T_{xy}$. Units mGalxEU.

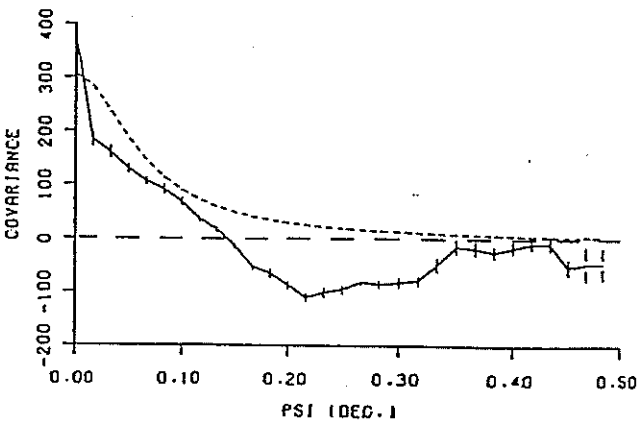

Fig. 9. Empirical and synthetic auto-covariance functions for the T_{yz} component. Units EU^2.

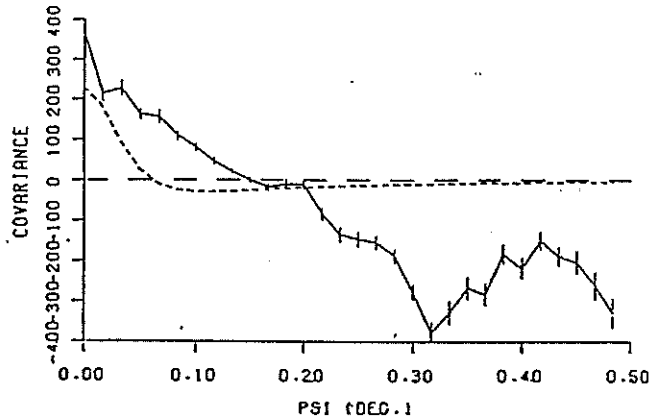

Fig. 10. Empirical and synthetic autocovariance functions for the $2*T_{xy}$ component. Units EU^2 .

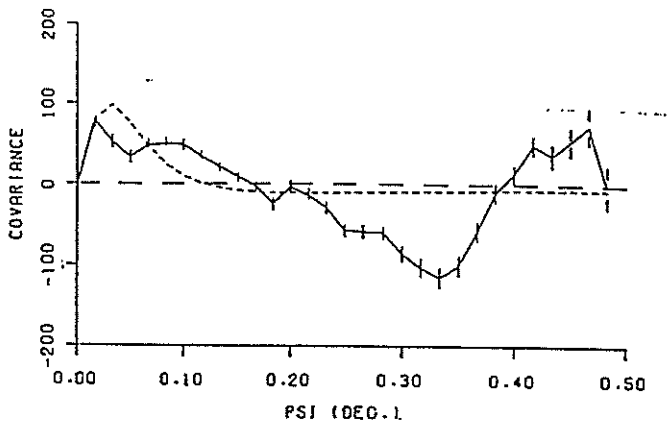

Fig. 12. Empirical and synthetic cross-covariance functions between T_{xy} and T_Δ. Units EU^2.

field through n linear functionals (equations (1)-(7)),

$$L_i(T) = y_i + e_i, \quad i = 1,\ldots,n$$

Here e_i is the noise or error. Then let C_{ij} denote the covariance between $L_i(T)$ and $L_j(T)$ and C_{Li} denote the covariance between the value of a linear functional L applied on the anomalous potential, L(T), and $L_i(T)$. We then obtain an estimate $L(\tilde{T})$ of L(T) as

$$L(\tilde{T}) = \{C_{Li}\}^T \{C_{ij} + D_{ij}\}^{-1} \{y_j\} \quad (8)$$

where D_{ij} is the covariance of the noise associated with the ith and jth observations. Let $\tilde{C}$ denote the sum of the C_{ij} and D_{ij} matrices. Then an estimate of the mean square error for a linear functional is obtained by

$$\sigma^2(L(\tilde{T})-L(T)) = C_{LL} - C_L^T \tilde{C}^{-1} C_L \quad (9)$$

where C_L is the vector of covariances between the observations and the quantity L(T) and C_{LL} is the variance of this quantity.

Similar equations are obtained if instead of the observations y, we use the values from which we have subtracted the effect of the topography or the contribution from a spherical harmonic expansion. On the right-hand side (of equation (8)) the covariance function will be the one associated with these residual observations. The vector of observations will consist of these residuals, and on the left-hand side we get the residual potential, to which in the final step we should add back the potential implied by the topography and the spherical harmonic expansion. In the case where we only have subtracted the contribution from GPM2, we will associate a superscript "s" with the relevant quantity, and if also the topographic effects have been subtracted, we will use the superscript "t", i.e., Δg^t.

The starting point for the use of LSC

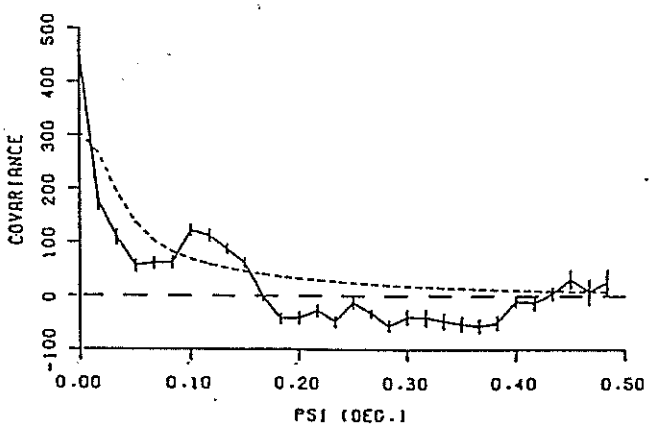

Fig. 11. Empirical and synthetic autocovariance functions for the T_Δ component. Units EU^2.

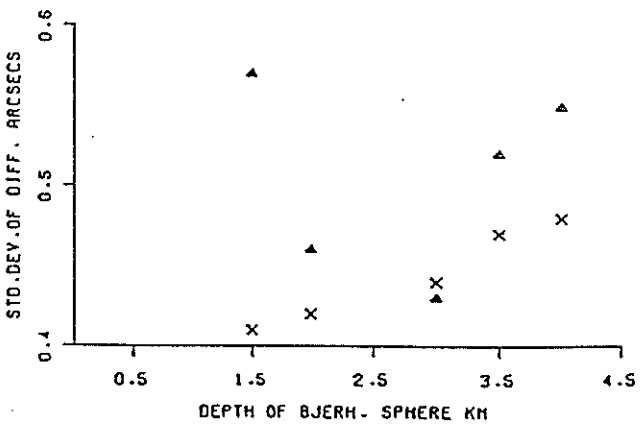

Fig. 13. Dependence of the prediction results (expressed in terms of standard deviations of the differences between observed minus predicted meridian (crosses) and prime vertical (triangles) deflections) on the depth to the Bjerhammar sphere. Topographic reduced data used.

TABLE 2. Prediction Results of the Two Components of the Deflection at Eight Points From 227 Gravity Points and of 12 Gravity Values From Deflection Values in 15 Points

Input Data	ξ, arc sec		η, arc sec		Δg, mGal	
	Mean	Standard Deviation	Mean	Standard Deviation	Mean	Standard Deviation
Unreduced	0.03	0.71	-0.17	0.43	5.20	4.32
Topographic reduced	-1.27	0.47	1.56	0.47	-	

in a local area is the computation and analytic modeling of the empirical covariance function. Its estimation is discussed in detail by Goad et al. (1984). Numerically, the estimation is simply done as the computation of the mean value of products of quantities lying within the same interval of spherical distance. The size of this interval is called the sampling interval.

For vector quantities, like components of deflections of the vertical, the components of the horizontal gravity (disturbance) gradient (equations (4) and (5)) and the mixed second-order derivatives (equations (6) and (7)), the products are formed between products of "along-track" and "cross-track" components. For details, see Krarup and Tscherning (1984).

The quality of the estimation depends on the size of the sampling error, the regularity of the data distribution, and the data error. The size of the area should also be so large that the mean value of the quantities (from which the contribution from the spherical harmonic expansion, here GPM2, have been subtracted), y_i^s, is zero. For a spherical harmonic expansion to degree 180, this generally will be achieved for a $1.5^\circ - 2^\circ$ equiangular area, since mean values of 1° blocks have been used for the computation of the coefficients.

For the approximately 1° block surrounding the torsion balance data the mean value of the available 227 Δg values is -3.3 mGal (see Table 1). Since the standard deviation is 19.8 mGal, this mean value is not statistically different from zero. The gravity values in this area were therefore used for the estimation of the covariance function, both using Δg^s and Δg^t values (see Figures 2 and 3).

When estimating cross-covariance functions with the torsion balance data, we have the problem that the data cover a much smaller area. Furthermore (see Table 1), the gravity variation in the $0.75^\circ \times 0.85^\circ$ area is significantly different from the variation in the area immediately surrounding the torsion balance data. Here the variation is much larger, and the mean values are nonzero. Anyway, we decided to estimate empirical autocovariance and cross-covariance functions between the (GPM2 and GPM2 + terrain reduced) gravity and torsion balance data. Figures 4-12 show the covariance functions for the GPM2 reduced data. It should be noted that the mean values have not been subtracted from the data.

The modeling of the empirical covariance function is based on the fitting of an analytic expression to the empirical values. We used a model for the gravity anomaly covariance function, developed by Tscherning and Rapp (1974),

$$C(P,Q) = \sum_{i=181}^{\infty} \frac{A(i-1)}{(i-2)(i+4)} \left[\frac{R_B^2}{rr'}\right]^{i+2} P_i(\cos\psi_{PQ}) \quad (10)$$

with the two free parameters A and R_B. In this expression, r' is the distance of the point Q from the origin, P_i the Legendre-polynomial of degree i, ψ_{PQ} the spherical distance between P and Q, and R_B the radius of the so-called Bjerhammar sphere. The summation starts from 181, since we have subtracted the effect of GPM2 to degree 180. This is equivalent to presupposing that the coefficients are error free, a hypothesis which is certainly not true. However, the consequence of adopting the hypothesis will mainly be seen in predicted geoid heights (see Arabelos, 1980). Also, the start of the summation from i=180 made it reasonable to introduce a modification, namely, the division by i+4 instead of a division by i+24 in equation (10), as recommended by Tscherning and Rapp (1974). This modification gives some computational savings.

A covariance function may be characterized by its value at spherical distance zero (the signal variance) and by the spherical distance where the covariance becomes equal to half the variance. This distance is called the correlation length.

The factor A in equation (9) is easily

TABLE 3. Prediction of Gravity Anomalies and Deflections of the Vertical From Torsion Balance Observations Using Least Squares Collocation

Input Components	Δg, mGal Mean	Δg, mGal Standard Deviation	ξ, arc sec Mean	ξ, arc sec Standard Deviation	η, arc sec Mean	η, arc sec Standard Deviation
Without Topographic Reduction, One Point per 2 arc min by 2 arc min Cell Used						
T_{xz}	10.43	22.45	-0.27	0.73	2.70	3.69
T_{yz}	4.97	4.87	-0.12	0.76	0.40	0.72
T_{Δ}	13.74	20.03	-0.95	1.70	2.51	3.17
$2*T_{xy}$	17.28	26.58	0.14	1.21	2.84	4.00
T_{xz},T_{yz}	0.79	3.40	-0.31	0.90	0.41	0.70
$T_{\Delta},2*T_{xy}$	16.85	14.94	-0.45	0.60	1.71	2.92
ALL	5.03	3.41	-0.04	0.74	0.18	0.56
Without Topographic Reduction, All Points Used						
T_{xz}	10.07	22.66	-0.20	0.91	2.62	3.88
T_{yz}	4.43	5.44	-0.12	0.50	0.55	0.47
T_{Δ}	12.68	19.26	-1.07	1.57	2.57	2.91
$2*T_{xy}$	17.59	24.38	0.28	1.21	2.72	3.98
T_{xz},T_{yz}	0.04	3.27	-0.20	1.08	0.68	0.52
$T_{\Delta},2*T_{xy}$	15.55	8.28	-0.24	1.07	1.37	2.71
ALL	-0.27	2.35	0.48	0.70	0.74	0.31
With Topographic Reduction, One Point per 2 arc min by arc min Cell Used						
	10.89	19.32	-1.54	0.44	3.74	3.64
T_{xz}	5.14	5.08	-1.32	1.07	1.83	0.87
T_{Δ}	14.13	16.13	-1.79	1.50	3.57	3.24
$2*T_{xy}$	16.79	24.03	-1.05	1.22	3.96	3.99
T_{xz},T_{yz}	1.51	2.74	-1.64	0.61	1.87	0.77
$T_{\Delta},2*T_{xy}$	16.44	13.21	-1.44	1.45	3.08	3.09
ALL	3.86	2.47	-1.50	0.58	1.75	0.71
With Topographic Reduction, All Points Used						
T_{xy}	10.64	19.37	-1.35	0.63	3.70	3.80
T_{yz}	4.15	5.37	-1.24	0.79	1.84	0.60
T_{Δ}	13.94	15.29	-1.89	1.39	3.65	3.11
$2*T_{xy}$	17.00	21.74	-0.89	1.27	3.88	3.94
T_{xz},T_{yz}	0.42	2.41	-1.41	0.80	1.95	0.56
T_{Δ} $2*T_{xy}$	15.91	7.21	-1.18	1.14	2.89	2.96
ALL	-0.93	1.71	-1.17	0.44	1.85	0.43

determined since it is linearly related to the variance. The value of R_B is related in a nonlinear manner to the the correlation distance (see Tscherning, 1985b, Figure 6). It is difficult to estimate due to the uncertainty in the estimation of the covariances. We decided to try to find the best value of R_B simply by carrying out prediction experiments with different values and then selecting the one which gave the best agreement between observed and predicted deflection values. The results are summarized in Figure 13. The depth to the Bjerhammar sphere found using this procedure was 3.0 km. Graphs of the covariance functions are shown

TABLE 4. Prediction Results Using All Torsion Balance Data and in Addition One Gravity Point and One Deflection Point and the Result Obtained by Badekas and Mueller(1968) Using Topographically Reduced Data and One Deflection Point

Input Data	Δg, mGal		ξ, arc sec		η, arc sec	
	Mean	Standard Deviation	Mean	Standard Deviation	Mean	Standard Deviation
Unreduced	0.05	2.15	0.26	0.68	0.02	0.30
Topographically reduced	-5.13	2.40	-0.06	0.49	0.55	0.61
Badekas and Mueller (1968)			0.23	0.42	-0.08	-0.31

with the empirical values in Figures 2-12.

It should be noted that this procedure of selecting a covariance function model could have been used if only torsion balance or gradiometer data had been available. A subset of the observations could have been used as test quantities, and the remaining observations could have been used as the given data. The covariance model that gave the best results in a least squares sense must then be the one in between the used set of models, which is closest to the true empirical covariance function. This follows implicitly from the definition of the empirical covariance function (see, e.g., Heiskanen and Moritz (1967, chapter 7)).

4. Prediction Tests and Results

For the evaluation of the predictions (equation (8)) as well as the calculation of error estimated (equation (9)) the FORTRAN program GEOCOL (Tscherning, 1985a) was used.

In order to check the consistency of the gravity vector data, we first predicted the deflections at the eight sites shown in Figure 1 from the 227 gravity values and, subsequently, the 12 gravity values in the vicinity of the torsion balance data from 15 pairs of deflection points in the same area as covered by the 227 gravity values. The results are given in Table 2. Note how well the gravity anomalies are determined from the deflections. Also note that the deflections are predicted just as well from the gravity data as from the torsion balance data, as we shall see later.

We also wanted to predict the torsion balance data from gravity and gravity and deflections from torsion balance data. We first assigned a noise standard deviation of 1.0 EU to the torsion balance data, equal to the value given by Badekas and Mueller (1968, p. 6871). However, all our results were "bad", in the sense that the error estimates computed using equation (9) were much smaller than the variance

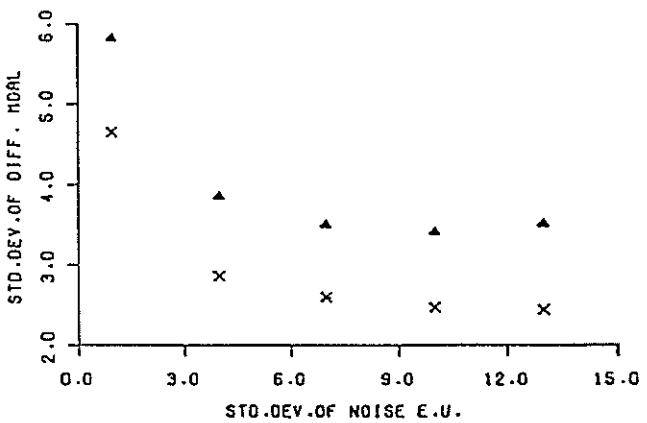

Fig. 14. The effect of changing of the noise level on the prediction results of gravity anomalies from torsion balance data. (Expressed in terms of standard deviation of differences observed minus predicted). Triangles, unreduced; crosses, topographic reduced data.

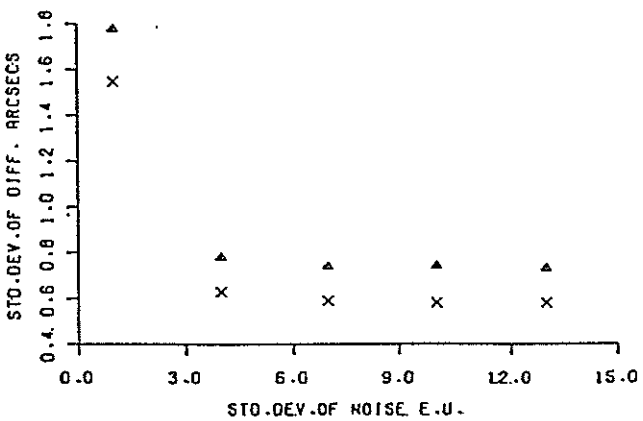

Fig. 15. The same effect as in Figure 14 for the ξ component of the deflection of the vertical.

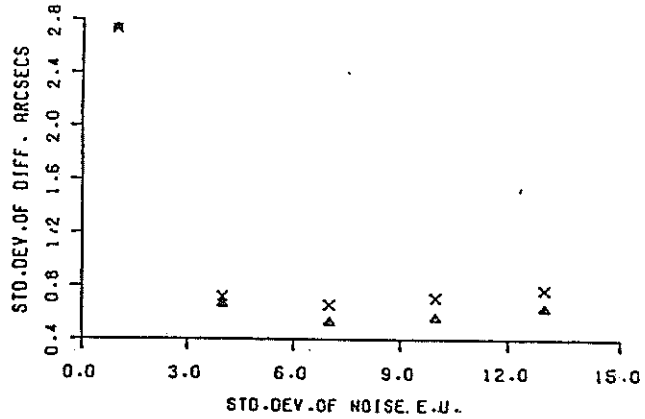

Fig. 16. The same effect as in Figure 14 for the η component of the deflection of the vertical.

of observed minus computed values. This made us go back to the publication Badekas (1967), which contains detailed maps showing the individual data in vectorlike form. This revealed that neighboring values could be rather different, signifying a much larger error level than we had expected. Also the empirically estimated autocovariance functions indicated that a rather large noise was present. This can be seen from Figures 8-11, where the variance is much larger (around 100 EU^2) than the value found by smoothly extrapolating from the first two to three empirical covariance values to the value at spherical distance zero (the variance). A value of 100 EU^2 is pessimistic but not impossible. Also one could argue that the large estimated variance comes from the signal itself. However, this would mean that the power spectrum should not go smoothly to zero like the degree raised to the power of -3 as used in equation (10) but would jump to some higher value after a certain degree.

Changing the noise variance to 100 EU^2, we obtained consistent results. We then tried changing noise levels. The results are illustrated in Figures 14-16. In fact, values of the noise between 50 and 150 EU^2 all give rather similar prediction results, but 100 EU^2 gave the best results. We then used this value in the following computations.

Having arrived this far, we decided to make a series of computational experiments, which should illustrate the dependence of the prediction result on (1) the model selected for the covariance function, (2) the use or nonuse of the topography, (3) the data type and the combination of various data types, and (4) the data density.

The dependence on the covariance function as already mentioned has been used to select a "best" analytic model. The dependence on the depth to the Bjerhammar sphere is illustrated in Figure 13. The variation of other parameters, such as the lower limit of the summation in equation (10), gave only small variations in the results.

The use of topographic data results in a slight smoothing of the gravity field data (see Table 1), and we should expect a similar improvement of the prediction results. However, as seen from Table 3, not very much is gained, but this is probably due to the high data density. The topographic information seems to be a priori well represented by the data.

In order to see the influence of the data density we used either all data points or one value from each 2 arc min by 2 arc min cell. Using all data gave only a small improvement, as seen from Table 3. More interesting is the clear difference in contribution from the various torsion balance components to the components of the gravity vector. As we should expect from geometrical reasons and from the results presented in Table 2, where gravity data were used to predict deflections, the horizontal gradients of the gravity disturbance contribu-

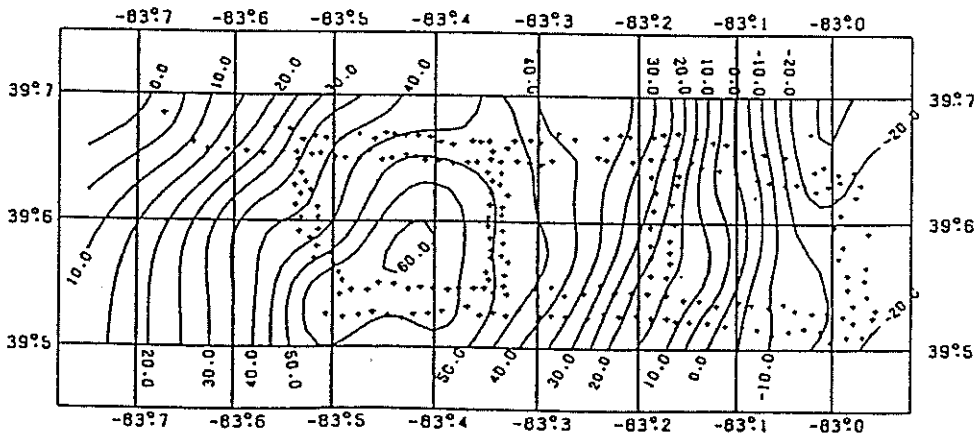

Fig. 17. Prediction of gravity anomalies from torsion balance data. (Contour interval is 5 mGal).

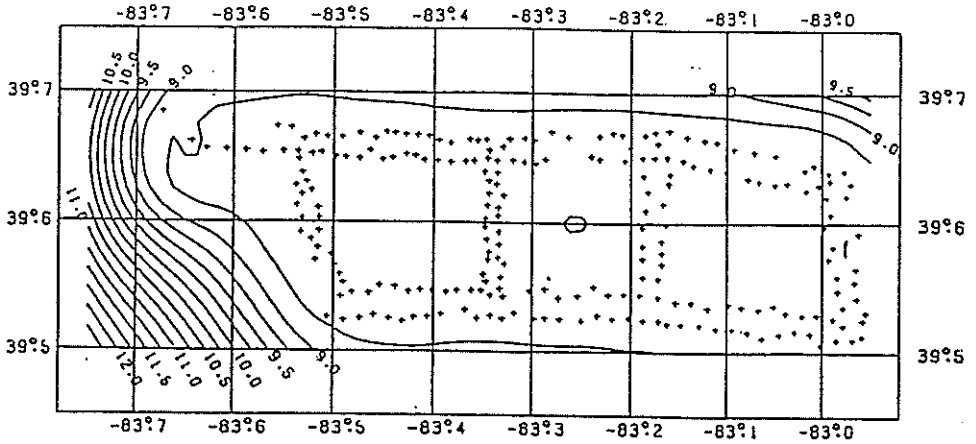

Fig. 18. Error of prediction of gravity anomalies from torsion balance data. (Contour line interval is 0.1 mGal).

te significantly to the determination of the deflection components. The second-order derivatives T_Δ and $2*T_{xy}$ contribute little of significance.

It is clear that we cannot estimate the absolute values of the gravity vector components from torsion balance data alone. This is also confirmed, since we get relatively large biases (see Table 3). However, gravity vector differences are well determined as seen from the small standard deviations in Table 3. On the other hand, we can easily add observed gravity vector information to the input data in LSC. We selected one of the deflection points, which coincides with one of the points of the torsion balance network, but we had to select a gravity station at some distance (1 km) from the network. The result is given in Table 4. We see that most of the biases have decreased, but the bias in the topographically reduced Δg has increased. The reason for this may, as mentioned, be due to the inconsistency of the topographic reductions.

Contour plots showing the predicted gravity anomaly and deflection components with the estimated errors of prediction (equation (9)) are shown in Figures 17-22. Only torsion balance data were used in the prediction. Note that the prime vertical deflection component (η) has a smaller estimated error in the middle of the area than the meridian component (ξ). This is due to the data distribution. Compare also the contours of the gravity map in Figure 1 (derived directly from the gravity data) with the contours of the map shown in Figure 17. The agreement is excellent.

5. Conclusion

We have shown that LSC is suitable for gravity vector estimation in a local area from gradiometerlike data. The results obtained in the best cases are 0.4 arc

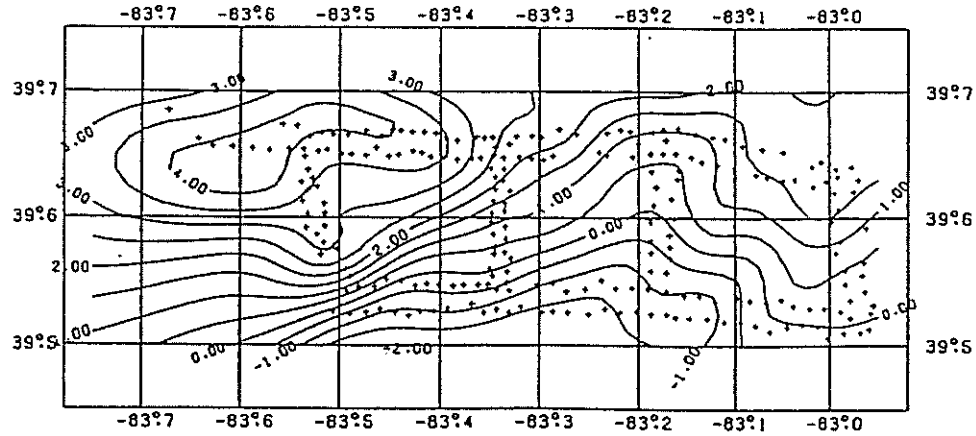

Fig. 19. Prediction of ξ from torsion balance data. (Contour interval is 0.5 arc sec).

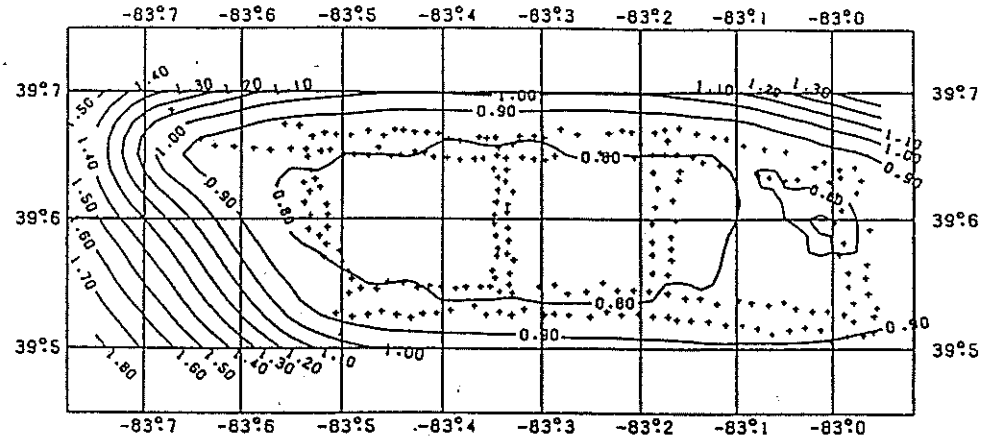

Fig. 20. Error of prediction of ξ from torsion balance data. (Contour interval is 0.1 arc sec).

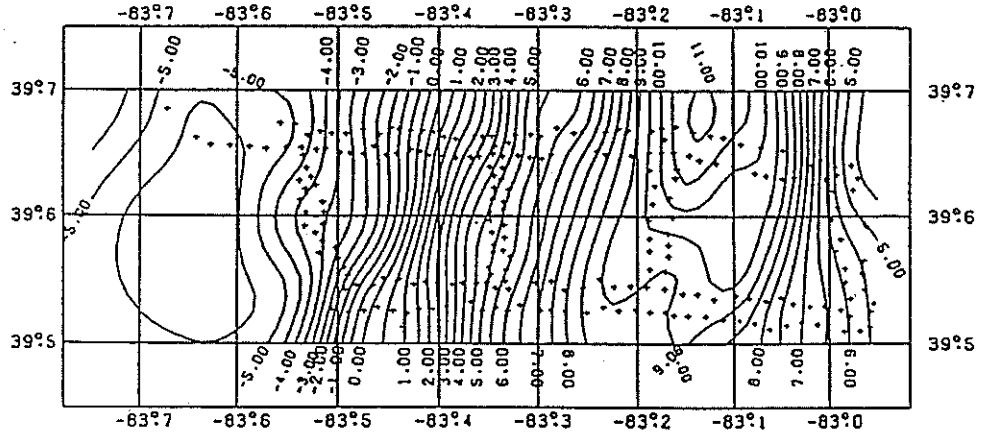

Fig. 21. Prediction of η from torsion balance data using equation (9). (Contour interval is 0.5 arc sec).

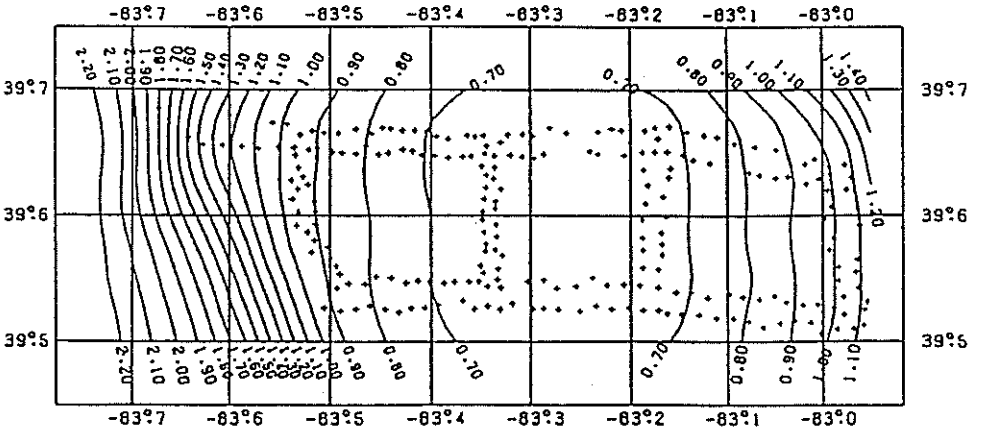

Fig. 22. Error of prediction of η from torsion balance data. (Contour interval is 0.1 arc sec).

sec for deflections and 1.6 mGal for gravity anomalies. With respect to the deflections this agrees with the result obtained by Badekas and Mueller (1968) using a completely different method, see Table 4. We are also in agreement with the results obtained by Hein (1981) for an area in Germany. This is very encouraging since we then may expect even better results using a gradiometer, which is supposed to have a noise level below 1 EU.

It is important to use a reasonable (correct) signed to noise ratio. This could for a given instrument (e.g., a gradiometer) be determined as here using data with a high signal to noise ratio.

The success of the prediction tests is also a further confirmation of the usefulness of the type of covariance function models (equation (10)) originally developed by Tscherning and Rapp (1974). Also the synthetic and empirically estimated covariances (see Figures 2-12) are in reasonable agreement, considering the limited geographical distribution of the torsion balance data.

Acknowledgement. This work was carried out while the first author was a visiting scientist at the Geodaetisk Institut, Denmark.

References

Arabelos, D.,Untersuchungen zur gravimetrischen Geoidbestimmung, dargestellt am Testgebiet Griechenland, Wissenchaftliche Arbeiten, Fachrichtung Vermess. der Univ. Hannover, Hannover, West Germany, 1980.

Badekas, J., Torsion balance observations in southwest Ohio, Rep. 89, Dep. of Geod. Sci., Ohio State Univ., Columbus, 1967.

Badekas, J., and I.I. Mueller, Interpolation of the vertical deflection from horizontal gravity gradients, J. Geophys. Res., 73, (22), 6869-6878, 1968.

Forsberg, R., A study of terrain reductions, density anomalies and geophysical inversion methods in gravity field modelling, Rep. 355, Dep. of Geod. Sci. and Surveying, Ohio State Univ. Columbus, 1984.

Goad, C.C., C.C. Tscherning, and M.M. Chin, Gravity empirical covariance values for the continental United States, J. Geophys. Res., 89, (B9), 7962-7968, 1984.

Hein, G., Untersuchungen zur terrestrischen Schweregradiometrie, Deutsche Geodätische Kommission, Reihe C, 264, Bayer. Akad. der Wiss., Munich, 1981.

Heiskanen, W.A., and H. Moritz, Physical Geodesy, W.H. Freemann, San Francisco, Calif., 1967.

Heiskanen, W.A., and U.A. Uotila, Gravity survey of the State of Ohio, Photogramm. Cartogr. Publ., 6, Inst. of Geod., Ohio State Univ., Columbus, 1956.

Jekili, C., On optimal estimation of gravity from gravity gradients at aircraft altitude, Rev. Geophys., 23, 301-311, 1985.

Krarup, T., and C.C. Tscherning, Evaluation of isotropic covariance functions of torsion balance observations, Bull. Geod., 58, (2), 180-192, 1984.

Mueller, I.I., and H.D. Preuss, Astrogeodetic deflections in southwest Ohio, Rep. 61, Dep. of Geod. Sci., Ohio State Univ., Columbus, 1965.

Rapp, R.H., The earth's gravity field to degree and order 180 using SEASAT altimeter data, terrestrial gravity data, and other data, Rep. 322, Dep. of Geod. Sci. and Surv., Ohio State Univ., Columbus, 1981.

Tscherning, C.C., GEOCOL-A FORTRAN-program for gravity field approximation by collocation, technical note, 3rd. ed., Geod. Inst., Charlottenlund, Denmark, 1985a.

Tscherning, C.C., Local approximation of the gravity potential by least squares collocation, Proceedings of the International Summer School on Local Gravity Field Approximation, Beijing, China, Aug. 21 - Sept. 4, 1984, edited by K.P. Szhwarz, Publ. 60003, pp. 277-362, Univ. of Calgary, Calgary Canada, 1985b.

Tscherning, C.C., and R.H. Rapp, Closed covariance expressions for gravity anomalies, geoid undulations and deflections of the vertical implied by anomaly degree variance models, Rep. 208, Dep. of Geod. Sci., Ohio State Univ., Columbus, 1974.

Wenzel, H.-G., Hochaufloesende Kugelfunktionsmodelle für das Gravitationspotential der Erde, Wissenchaftlische Arbeiten, Fachrichtung Vermess. der Univ. Hannover, Hannover, West Germany, 1985.

D. Arabelos, Department of Geodesy and Surveying, University of Thessaloniki, Thessaloniki 54006, Greece.

C.C. Tscherning, Geodaetisk Institut, Geodetic Department I, DK-2920 Charlottenlund, Denmark.

(Received September 24, 1986;
revised March 23, 1987
accepted March 25, 1987.)